ChemComm

COMMUNICATION

View Article Online
View Journal | View Issue

Cite this: *Chem. Commun.*, 2021, **57**, 4130

Received 25th February 2021,
Accepted 10th March 2021

DOI: 10.1039/d1cc01064f

rsc.li/chemcomm

Folding of phosphodiester-linked donor–acceptor oligomers into supramolecular nanotubes in water†

Kévan Pérez de Carvasal,[a] Nesrine Aissaoui,[b] Gérard Vergoten,[c] Gaëtan Bellot,[b] Jean-Jacques Vasseur,[a] Michael Smietana *[a] and François Morvan *[a]

Inspired by the automated synthesis of DNA on a solid support, the electron-rich dialkoxynaphthalene (DAN) donor and the electron-deficient naphthalene-tetracarboxylic diimide (NDI) acceptor, amphiphilic foldamers have been synthesised from their respective phosphoramidite building blocks. The folding of the phosphodiester-linked hexamer (DAN–NDI)$_3$ revealed the formation of regular supramolecular nanotubes in water resulting from the self-assembly of multiple hexamers stabilized by donor/acceptor interactions and the solvophobic effect.

The tridimensional structure of supramolecular assemblies plays an important role in their biophysical properties and ultimately their functions regardless of whether they are natural (DNA, proteins) or synthetic (molecular machines, polymers). In the quest for new folded structures and ultimately in tuning their structural conformation to control their function, foldamers have emerged as new tools for the development of biologically active synthetic molecules.[1] Foldamers are linear artificial oligomers that are able to fold into secondary structures stabilized by non-covalent forces including hydrogen bonds, ionic interactions, π–π or σ–π interactions, van der Waals forces or solvophobic driving force in water.[2] While DNA itself can be seen as a foldamer,[3–5] several examples of folded DNA-inspired oligomers have been reported in the literature. These structures are generally composed of repetitive aromatic[6] polypyrene,[7–13] polyanthracene[14] or polyphenanthrene[15] units, except one built from perylenediimide–pyrene supramolecular interactions,[16] which induce the formation of supratubular polymers or nanosheets. Along this line, foldamers built on electrostatic complementarity interactions (donor/acceptor) in water are particularly important for the elaboration of novel materials, which are able to interfere with biological aqueous systems. Iverson and co-workers have described the synthesis of self-complexing systems based on 1,5-dialkoxynaphthalene (DAN) and 1,8,4,5-naphthalenetetracarboxylic diimide (NDI) motifs linked together with L-aspartic acid[17–19] or with mixed amino-acids to impart aqueous solubility.[20] Both aromatic units are stabilized in water by the solvophobic[21] effect and donor–acceptor interactions known as charge-transfer (CT).[22–25] Alternatively, CT-based foldamers built from DAN and pyromellitic diimide units and tetra- or hexaethylene glycol linkers complexed with alkali metals have also been reported.[26]

Herein, we present the synthesis and supramolecular assembly of new water-soluble DNA-inspired foldamers built from DAN and NDI moieties linked by negatively charged phosphodiesters leading to the formation of nanotubes in water without the need of an organic solvent or any type of adjuvant (Fig. 1).

The synthesis of these new structures started with the preparation of NDI and DAN phosphoramidite building blocks able to be directly assembled on an automated DNA synthesizer. This chemical approach allows rapid access to various foldamer sequences.[27]

The synthesis of NDI phosphoramidite **4** was proceeded by reacting naphthalene dianhydride **1** with 3 equiv. of 3-aminopropanol to give the corresponding diimide **2** in 97% yield (Scheme 1).[28] Compound **2** was then treated with 1 equiv. of DMTrCl to give the monotritylated derivative **3** in a rather modest yield (38%) due to the formation of a large amount of the ditritylated

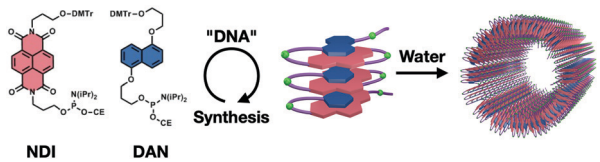

Fig. 1 Schematic representation of a nanotube built from the supramolecular assembly of (DAN–NDI)$_3$ foldamers.

[a] *Université de Montpellier, CNRS, ENSCM, Institut des Biomolécules Max Mousseron, Montpellier, France. E-mail: francois.morvan@umontpellier.fr, michael.smietana@umontpellier.fr*
[b] *Université de Montpellier, INSERM, CNRS, Centre de Biochimie Structurale, Montpellier, France*
[c] *Université de Lille, Inserm, INFINITE – U1286, Institut de Chimie Pharmaceutique Albert Lespagnol (ICPAL), Faculté de Pharmacie, 3 rue du Professeur Laguesse, Lille 59006, France*

† Electronic supplementary information (ESI) available. See DOI: 10.1039/d1cc01064f

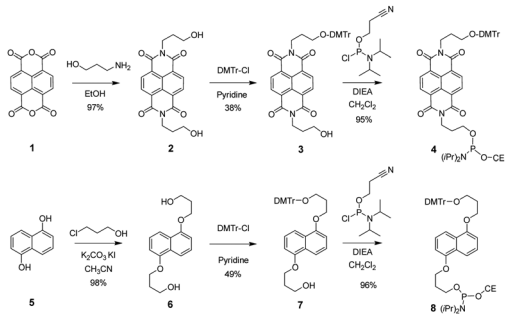

Scheme 1 Synthesis of NDI **4** and DAN **8** phosphoramidites.

side product. Finally, phosphitylation of **3** using *N*, *N*-diisopropylcyanoethyl chlorophosphine gave NDI phosphoramidite **4** in 95% yield and an overall yield of 35%.

Concerning DNA phosphoramidite **8**, any attempts to use standard *O*-alkylation methods of 1,5-dihydroxynaphthalene **5** described in the literature were unsatisfactory and gave the expected dialkyl derivative **6** in low yield (20 to 45%) along with the formation of an oxidized side product.[29,30] Hence the alkylation was performed with 4 equiv. of 3-chloropropanol in the presence of K_2CO_3 and KI in acetonitrile under reflux in an atmosphere of argon for 18 h. Under these conditions, derivative **6** was isolated as a clean yellow-green powder in nearly quantitative yield. Following the two-step protocol described for the synthesis of **4**, the DAN phosphoramidite **8** was obtained in 46% overall yield.

With these phosphoramidites in hand, monomers of DAN **9** and NDI **10**, as controls, as well as the alternated dimer **11** and hexamer **12** were synthesized on a DNA synthesizer using phosphoramidite chemistry and a custom-made propanediol solid support (Scheme 2). To assure water solubility, an additional phosphodiester linkage was added at the end of each sequence using a propanediol phosphoramidite unit **13**.

After elongation, a methanolic ammonia treatment was applied to deprotect and release compounds **9–12** from the solid support. They were purified by C_{18} RP HPLC and characterized by MALDI-TOF mass spectrometry (Table S1 and Fig. S1–S4, ESI†).

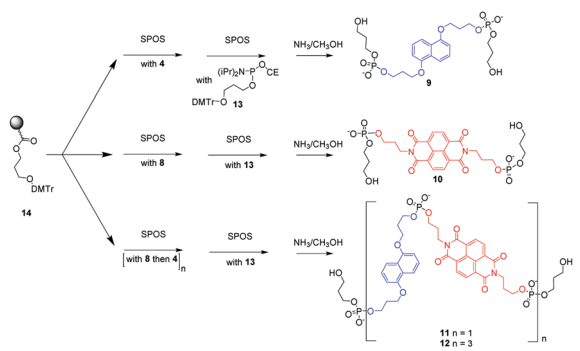

Scheme 2 Synthesis of monomers **9** and **10**, and foldamers **11** and **12**. SPOS: solid-phase oligonucleotide synthesis. SPOS conditions: (1) 3% trichloroacetic acid (TCA) in CH_2Cl_2; (2) phosphoramidite derivative + benzylthiotetrazole (BTT); (3) Ac_2O, *N*-Me-imidazole, 2,6-lutidine; (4) 0.1 m I_2 THF/H_2O/pyridine.

Compounds **9–11** were first analyzed using ^{1}H-NMR spectroscopy (Fig. S5, ESI†). The DAN derivative **9** displays three types of aromatic signals, 2 doublets and a triplet between 7.1 and 8.0 ppm, while the NDI derivative **10** displays only one single aromatic signal at 8.75 ppm due to its symmetry. Compound **11** reveals multiple signals due to the asymmetry of the molecule which leads to a polarization of the aromatics, thus confirming their interaction. When the temperature was increased from 25 to 85 °C, a change of the folding state of **11** was observed. At 25 °C, DAN and NDI aromatic protons exhibited a lower chemical shift which indicates a strong shielding suggesting that **11** is strongly folded on itself. When the temperature was increased up to 85 °C, the strong deshielding of the aromatic protons was progressively apparent. Indeed, the two doublets of NDI aromatics moved closer together indicating a lower differentiation of the hydrogen atoms as a result of fewer interactions between DAN and NDI (Fig. S6, ESI†). In addition, the solution at high temperature still exhibited pink color visible to the naked eye, which is indicative of the presence of a CT-band. This study demonstrates that increasing the temperature does not unfold the structure completely.

Fig. 2 shows the UV/visible absorption spectra of the mathematical sum of **9** and **10** (both at 99 μM) as well as **12** (33 μM) in aqueous solution. The spectrum of **12** displayed an attenuation of the absorption bands, a change of the two NDI intensity bands and a 37% hypochromicity in comparison with the mathematical sum of **9** and **10**. The charge transfer band is centered at 530 nm with a molar extinction coefficient of 300 M^{-1} cm^{-1}, but a higher concentration is needed to clearly observe it (see Fig. 2, inset). The study performed at 85 °C displayed a very similar spectrum with a slight decrease of the CT band intensity demonstrating the strong folding of **12** (Fig. S7, ESI†). All these changes are characteristic of a folded structure and similar to those observed for previously reported DAN/NDI foldamers.[20,26,31] However, in contrast to DAN/NDI foldamers built with amino acids,[20] the current foldamer was very stable and insensitive to temperature variations.

The fluorescence emission spectrum of compound **12** was compared with the emission spectra of **9** and **10** (Fig. S8, ESI†). Emissions of **9** and **10** concur with previous studies reporting two high emissions of fluorescence at 330 and 345 nm[18,32] for **9** (λ_{ex} = 296 nm) and two high emissions of fluorescence at 390

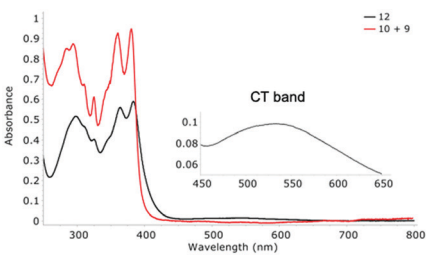

Fig. 2 UV-vis spectra of oligomer **12** (33 μM, black curve) in water and the mathematical sum of **9** and **10** (99 μM, red curve). Inset: Expanded region of the charge-transfer band of **12** at 100 μM.

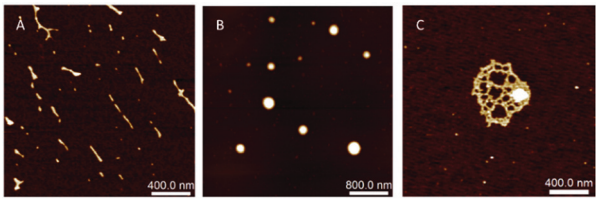

Fig. 3 AFM images (height) at 45 μM in water after 1 d: (A) **9**, (B) **10** and (C) **9 + 10**.

and 420 nm[33] for **10** (λ_{ex} = 363 nm). As expected, **12** exhibits a very low emission of fluorescence at both excitation wavelengths due to the stable folding of the DAN and NDI units with charge transfer that induces a very fast non-radiative decay.[32] The pink color which is characteristic of the CT interaction observed for **12**, associated with the important hypochromicity observed in UV-vis spectra as well as the strong decrease of fluorescence emission, confirmed the presence of a folded structure.

The structures of the different compounds (**9**, **10**, **9 + 10**, **11** and **12**) were imaged using atomic force microscopy (AFM) in tapping-mode. Monomers alone dissolved in water (45 μM), for 1 day, form quite different structures. The DAN derivative **9** forms nanotubes (up to several hundreds of nm in length and ~2 nm in height) with some ramifications (Fig. 3A and Fig. S9, ESI†), while the NDI derivative **10** forms vesicles (~30–200 nm in diameter) (Fig. 3B and Fig. S10, ESI†). When both compounds were mixed together in water, we observed strongly ramified nanotubes with a length of several hundreds of nm and a height of ~1.5 nm (Fig. 3C and Fig. S11, ESI†).

Dimer **11** was studied at a concentration of 45 μM after one day in water. Only a very few nanotubes with a length up to 1 μm and heights between 0.5 and 1.2 nm were observed (Fig. S12, ESI†).

Then, the folding of hexamer **12** was studied according to its concentration and time of storage in solution. At 1 μM, we observed only a few single nanotubes that are around 200–300 nm long and also ramified nanotubes that are up to 1 μm long with heights between 1 and 1.5 nm (Fig. S13, ESI†). When the concentration was increased to 15 μM, more regular and homogeneous nanotubes (100–400 nm long, 2 nm height) were visualized (Fig. 4A and Fig. S14, ESI†) and at 30 μM even longer nanotubes (200–500 nm long, 2 nm height) were observed. Interestingly two nanotubes on top of each other were also detected (Fig. S15, ESI†). The sample at a concentration of 15 μM was then studied after 3 and 7 days to monitor any changes over time (Fig. S16, ESI†). Nanotubes with a similar width but a much higher length greater than 1 μm were observed (Fig. 4C and D). Interestingly, when the 3 day old solution was heated to 80 °C for 1 h, we observed the presence of smaller structures, indicating a disassembly of the nanotubes upon heating (Fig. S17, ESI†). From the amplitude AFM images, we could observe that this structure is a collapsed nanotube with a thickness of 2 nm and a width of 16 nm (Fig. 4B). These nanotubes have a similar structure to polyanthracenes reported by Häner.[11]

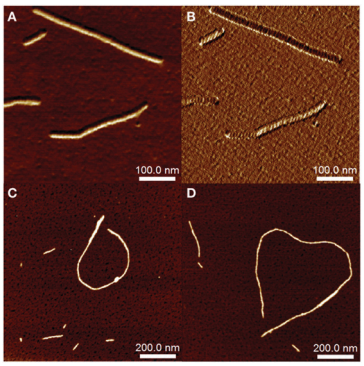

Fig. 4 AFM images of **12** at 15 μM in water: (A) 1 d, height, (B) 1 d, amplification, (C) 3 d, height, and (D) 7 d, height.

The formation of nanotubes for **12** was confirmed by TEM imaging. A first study performed in water with the addition of 2% uranyl acetate solution for staining showed that the nanofibers folded on themselves to form a ball of twisted nanotubes (Fig. S18, ESI†). Uranyl ions are known to bind with nucleic acid phosphates and to induce aggregation.[34] To reduce the formation of related artifacts from uranyl acetate staining, we adapted the buffer sample by adding 10 mM phosphate buffer pH 7 and 10 mM NaCl. The TEM micrographs of the 15 μM sample in this buffer showed micron scale one-dimensional nanotubes similar to AFM images with fewer defects (Fig. 5 and Fig. S19, ESI†).

According to the AFM study, foldamer **12** forms nanotubes with an approximate thickness of 8 to 10 nm and lengths of several micrometers. The molecular modelling study of foldamer **12** shows a size of one unit of foldamer that is about ~2 nm long and ~1.6 nm wide with a distance between two aromatics of about 3.5 Å (Fig. 6A). The AFM images show collapsed tubes with a section around ~16 nm and a height of ~2 nm. In line with the work of Häner *et al.*,[11] the height, measured by AFM, corresponds to two layers of foldamers indicating that the thickness of one layer is ~1 nm corresponding roughly to the length of aromatic motifs with a part of the propyl arms. Hence, the tube has a perimeter of ~32 nm corresponding to 16 hexamers and a diameter of ~10 nm was also observed by TEM. The molecular modeling conducted with these parameters with four turns is shown in Fig. 6B. We calculated the longitudinal and lateral potential energies of the interaction of two foldamers as −32.5 kcal mol^{-1} and −76.2 kcal mol^{-1}, respectively, corresponding to the energy

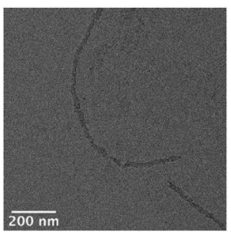

Fig. 5 Negative-stained TEM images of **12** in 10 mM phosphate buffer pH 7 and 10 mM NaCl, 15 μM 1 d.

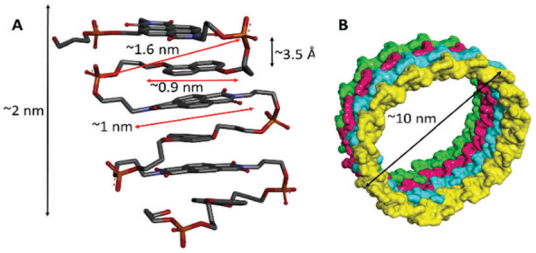

Fig. 6 (A) Molecular modeling of **12**, (B) modeling of four turns of the tube with 16 units by turn and an ~10 nm diameter.

allowing the elongation of the fiber adding several units stabilized by the CT interaction and to the energy allowing the lateral interaction of the twisted fiber to close the tube (Fig. S20, ESI†).

In conclusion, we provide an easy method for the synthesis of new donor–acceptor amphiphilic phosphodiester foldamers, fully soluble in water, without any cosolvent, stabilized by a variety of interactions, *i.e.*, electronic complementary, charge transfer and solvophobic effects. Starting from DAN and NDI phosphoramidites as building blocks, we successfully synthesized a $(DAN–NDI)_3$ hexamer and demonstrated its folding by UV-visible and fluorescence studies. AFM and TEM characterizations allowed us to visualize the formation of regular nanotubes that are several hundreds of nanometers in length and ~10 nm in diameter resulting from a supramolecular arrangement of several hexamers stabilized by longitudinal and lateral interactions. In contrast to Iverson and co-workers who observed an amyloid-like behavior for the alternated DAN and NDI foldamers linked with amino acids when heated,[20] we demonstrated that alternated DAN and NDI foldamers linked by phosphodiesters are stable even at high temperature and are able to form nanotubes, thanks to strong CT stabilization in water. However, the nanotubes can be destroyed by heating to 80 °C. In addition, the structuring of these original foldamers triggered by charge-transfer interactions complements a range of bio-inspired architectures based on π-stacking interaction reported by Häner with polypyrene,[7–13] polyanthracene[14] or polyphenanthrene.[15] Furthermore, our current foldamers are fully soluble in water without the addition of any organic solvent which makes them compatible in aqueous media under physiological conditions.

Current water-soluble DNA-inspired foldamers open the way to new objects that could be decorated with motifs recognized by living systems to develop biologically active synthetic molecules or new hybrid materials.

K. P. C. thanks the Univ. of Montpellier (UM) for the award of a research studentship. F. M. is a member of Inserm. We thank Dr F. Menges (Univ. of Konstanz) for the use of SpectraGryph software. We also thank the *Centrale de Technologie en Micro et nanoélectronique* of the UM for AFM analyses.

Conflicts of interest

There are no conflicts to declare.

References

1 G. Guichard and I. Huc, *Chem. Commun.*, 2011, **47**, 5933–5941.
2 D. J. Hill, M. J. Mio, R. B. Prince, T. S. Hughes and J. S. Moore, *Chem. Rev.*, 2001, **101**, 3893–4012.
3 P. D. S. Hecht and D. I. Huc, *Foldamers: Structure, Properties, and Applications*, Wiley-VCH, 2007, pp. 291–329, DOI: 10.1002/9783527611478.ch10.
4 V. Berl, I. Huc, R. G. Khoury, M. J. Krische and J.-M. Lehn, *Nature*, 2000, **407**, 720–723.
5 P. D. S. Hecht and D. I. Huc, *Foldamers: Structures, properties, applications*, Wiley-VCH, 2007, pp. 1–435, DOI: 10.1002/9783527611478.ch1.
6 M. Vybornyi, Y. Vyborna and R. Häner, *Chem. Soc. Rev.*, 2019, **48**, 4347–4360.
7 R. Häner, F. Samain and V. L. Malinovskii, *Chem. – Eur. J.*, 2009, **15**, 5701–5708.
8 R. Häner, F. Garo, D. Wenger and V. L. Malinovskii, *J. Am. Chem. Soc.*, 2010, **132**, 7466–7471.
9 M. Vybornyi, A. V. Rudnev, S. M. Langenegger, T. Wandlowski, G. Calzaferri and R. Häner, *Angew. Chem., Int. Ed.*, 2013, **52**, 11488–11493.
10 Y. Vyborna, M. Vybornyi, A. V. Rudnev and R. Häner, *Angew. Chem., Int. Ed.*, 2015, **54**, 7934–7938.
11 M. Vybornyi, Y. Bur-Cecilio Hechevarria, M. Glauser, A. V. Rudnev and R. Häner, *Chem. Commun.*, 2015, **51**, 16191–16193.
12 M. Vybornyi, A. Rudnev and R. Häner, *Chem. Mater.*, 2015, **27**, 1426–1431.
13 Y. Vyborna, M. Vybornyi and R. Haner, *Chem. Commun.*, 2017, **53**, 5179–5181.
14 H. Yu and R. Häner, *Chem. Commun.*, 2016, **52**, 14396–14399.
15 C. D. Bosch, S. M. Langenegger and R. Haner, *Angew. Chem., Int. Ed.*, 2016, **55**, 9961–9964.
16 C. B. Winiger, S. M. Langenegger, O. Khorev and R. Haner, *Beilstein J. Org. Chem.*, 2014, **10**, 1589–1595.
17 R. Scott Lokey and B. L. Iverson, *Nature*, 1995, **375**, 303.
18 A. J. Zych and B. L. Iverson, *J. Am. Chem. Soc.*, 2000, **122**, 8898–8909.
19 B. A. Ikkanda and B. L. Iverson, *Chem. Commun.*, 2016, **52**, 7752–7759.
20 C. Peebles, R. Piland and B. L. Iverson, *Chem. – Eur. J.*, 2013, **19**, 11598–11602.
21 M. S. Cubberley and B. L. Iverson, *J. Am. Chem. Soc.*, 2001, **123**, 7560–7563.
22 M. W. Hanna and A. L. Ashbaugh, *J. Phys. Chem.*, 1964, **68**, 811–816.
23 D. A. Deranleau, *J. Am. Chem. Soc.*, 1969, **91**, 4050–4054.
24 A. Das and S. Ghosh, *Angew. Chem., Int. Ed.*, 2014, **53**, 2038–2054.
25 M. Kumar, K. Venkata Rao and S. J. George, *Phys. Chem. Chem. Phys.*, 2014, **16**, 1300–1313.
26 S. Ghosh and S. Ramakrishnan, *Angew. Chem., Int. Ed.*, 2004, **43**, 3264–3268.
27 S. L. Beaucage and M. H. Caruthers, *Tetrahedron Lett.*, 1981, **22**, 1859–1862.
28 N. Rahe, C. Rinn and T. Carell, *Chem. Commun.*, 2003, 2120–2121.
29 P. Talukdar, G. Bollot, J. Mareda, N. Sakai and S. Matile, *J. Am. Chem. Soc.*, 2005, **127**, 6528–6529.
30 R. Kamiński, J. Kowalski, I. Mames, B. Korybut-Daszkiewicz, S. Domagała and K. Woźniak, *Eur. J. Inorg. Chem.*, 2011, 479–488.
31 V. J. Bradford and B. L. Iverson, *J. Am. Chem. Soc.*, 2008, **130**, 1517–1524.
32 P. R. Ashton, R. Ballardini, V. Balzani, S. E. Boyd, A. Credi, M. T. Gandolfi, M. Gomez-Lopez, S. Iqbal, D. Philp, J. A. Preece, L. Prodi, H. G. Ricketts, J. F. Stoddart, M. S. Tolley, M. Venturi, A. J. P. White and D. J. Williams, *Chem. – Eur. J.*, 1997, **3**, 152–170.
33 B. Abraham, S. McMasters, M. A. Mullan and L. A. Kelly, *J. Am. Chem. Soc.*, 2004, **126**, 4293–4300.
34 M. L. Watson, *J. Biophys. Biochem. Cytol.*, 1958, **4**, 475–478.